Journal of the Korean Ceramic Society
Vol. 52, No. 5, pp. 331~337, 2015.

http://dx.doi.org/10.4191/kcers.2015.52.5.331

Effect of B-Cation Doping on Oxygen Vacancy Formation and Migration in $LaBO_3$: A Density Functional Theory Study

Hyunguk Kwon, Jinwoo Park*, Byung-Kook Kim, and Jeong Woo Han†**

Department of Chemical Engineering, University of Seoul, Seoul 02504, Korea
**Graphene Research Institute and Department of Physics, Sejong University, Seoul 05006, Korea*
***High Temperature Energy Materials Center, Korea Institute of Science and Technology, Seoul 02792, Korea*

(Received July 27, 2015; Revised August 19, 2015; Accepted August 31, 2015)

ABSTRACT

$LaBO_3$ (B = Cr, Mn, Fe, Co, and Ni) perovskites, the most common perovskite-type mixed ionic-electronic conductors (MIECs), are promising candidates for intermediate-temperature solid oxide fuel cell (IT-SOFC) cathodes. The catalytic activity on MIEC-based cathodes is closely related to the bulk ionic conductivity. Doping B-site cations with other metals may be one way to enhance the ionic conductivity, which would also be sensitively influenced by the chemical composition of the dopants. Here, using density functional theory (DFT) calculations, we quantitatively assess the activation energies of bulk oxide ion diffusion in $LaBO_3$ perovskites with a wide range of combinations of B-site cations by calculating the oxygen vacancy formation and migration energies. Our results show that bulk oxide ion diffusion dominantly depends on oxygen vacancy formation energy rather than on the migration energy. As a result, we suggest that the late transition metal-based perovskites have relatively low oxygen vacancy formation energies, and thereby exhibit low activation energy barriers. Our results will provide useful insight into the design of new cathode materials with better performance.

Key words : Solid oxide fuel cell cathode, Oxide ion transport, Oxygen vacancy formation, Oxygen vacancy migration, Density functional theory

1. Introduction

Solid oxide fuel cells (SOFCs), one of several powerful solutions to the problems of fossil fuels, are solid-state devices that generate electricity through the direct conversion of chemical fuels under high temperature.[1-3] SOFCs provide many advantages over other fuel cells, including high efficiency and fuel flexibility; further, SOFCs do not require expensive catalysts such as platinum. On the other hand, the high operating temperature of SOFCs leads to material degradation and sealing difficulties. Reduction in operating temperature is therefore an important challenge for high performance SOFCs.[4] Unfortunately, at reduced temperatures, the deterioration of the oxygen reduction reaction (ORR) rate on the cathode side becomes a limiting factor in SOFCs.[5] To solve the issue, mixed ionic-electronic conductors (MIECs) based on perovskites are regarded as promising cathode materials.[6-8] These MIEC cathodes extend the ORR active sites by allowing fast ionic transport because oxygen reduction can occur along the gas/cathode interface as well as at the triple phase boundary. This effect consequently enhances the surface exchange rate, which is a key factor in ORR activity.[9-11] Hence, it is necessary to design cathode materials with high ionic conductivity.

Although there are several ways of enhancing ionic conductivity, such as using a new class of materials (the double[12,13] or layered perovskites[14,15]) or introducing strain,[16-20] the optimization of compositions in simple perovskites by fully or partially substituting A or B cations can be a powerful method with regard to overall convenience and efficiency. For example, Sc doping in the B-sites of LSM leads to faster oxide ion transport when Sc concentration is lower than 5 mol%.[21] Furthermore, the oxygen self-diffusion coefficient of $La_{1-x}Sr_xCo_{1-y}Fe_yO_{3-\delta}$ is several orders of magnitude higher than that of $La_{0.8}Sr_{0.2}MnO_3$ at even lower operation temperature.[22,23] These reports show that ionic conductivity can be made tunable simply by changing the composition.[24]

In this study, therefore, to elucidate the role of substitutions at B-sites, we examine the bulk oxide ion diffusion coefficient in $LaB_xB'_{1-x}O_{3-\delta}$ (B, B' = Cr, Mn, Fe, Co, and Ni). Cherry *et al.*[25] demonstrated that a hopping mechanism, due to its low energy barriers in oxide ion diffusion, is strongly preferred over an interstitial mechanism. Thus, the self-diffusion coefficient (D_o) shows an Arrhenius form dependence on temperature, as follows[26-28]

$$D_o = Ae^{-(E_{vac}+E_{mig})/k_BT},$$

where E_{vac} and E_{mig} are the oxygen vacancy formation energy and the oxygen vacancy migration energy barrier, respectively, and A is a pre-exponential factor. From the

†Corresponding author : Jeong Woo Han
E-mail : jwhan@uos.ac.kr
Tel : +82-2-6490-2373 Fax : +82-2-6490-2364

equation, we can calculate the activation energy in oxide ion diffusion using the sum of E_{vac} and E_{mig}. This provides valuable information for improving the oxide ion diffusion rates: high oxygen vacancy concentration (lower E_{vac}) and low intrinsic migration barrier energy of oxygen vacancy (lower E_{mig}) in bulk perovskite can enhance the oxide ion diffusivity.

2. Experimental Procedure

Our density functional theory (DFT) calculations were performed with the Vienna *Ab initio* Simulation Package (VASP).[29,30] We employed the Perdew-Burke-Ernzerhof (PBE) functional based on the generalized gradient approximation (GGA).[31] All calculations used a plane wave expansion with a cutoff of 400 eV and included spin polarization. Geometries were relaxed using a conjugate gradient algorithm until the forces on all unconstrained atoms were less than 0.03 eV/Å. Because self-interaction errors occur in the traditional DFT with GGA for strongly correlated electronic materials,[32] we considered the DFT+U method proposed by Dudarev[33] with U_{eff} = 3.5 eV (Cr), 4.0 eV (Mn), 4.0 eV (Fe), 3.3 eV (Co), and 6.4 eV (Ni).[34] For the bulk calculations, a pseudocubic 2 × 2 × 2 supercell containing 40 atoms and a Monkhorst-Pack[35] grid of 4 × 4 × 4 *k*-points were used. Although the magnetic structures of $LaBO_3$ change depending on the B-site cations, we chose the ferromagnetic (FM) state for all bulk calculations. According to previous studies,[36-38] this approach does not qualitatively alter the trends of the oxygen vacancy formation energies or the migration energies.

The formation energy of an oxygen vacancy was calculated by

$$E_{vac}(eV) = E_{defect} - E_{perfect} + \frac{1}{2}E_{O_2}$$

where E_{defect} and $E_{perfect}$ are the total energies of one vacancy-defected (δ =0.125) and perfect structures, respectively and E_{O_2} is the total energy of O_2 in the gas phase. For the calculations of the total energy of O_2, the molecular geometries were optimized in the large periodically repeated cubic boxes (approximately 20 Å on a side).[39] The lattice constants of the defective structures were used equally with those of the perfect structures because the change in lattice constants due to the formation of oxygen vacancies is negligible at relatively low oxygen vacancy concentrations.[26,40,41]

The migration barrier of an oxygen atom (or an oxygen vacancy) was calculated using the climbing image-nudge elastic band (CI-NEB) method.[42] We applied three intermediate images to accurately determine the minimum energy pathway.[16,37,43,44] The NEB simulations were performed at fixed lattice vectors with internal relaxation.

3. Results and Discussion

3.1. Oxygen vacancy formation

In this study, there are three cases of perovskite bulk structures classified as a function of composition of B-site cations (Fig. 1). While $LaBO_3$ (B-V_O-B) and $LaB_{0.50}B'_{0.50}O_3$ (B-V_O-B') have only one distinguishable oxygen vacancy site, $LaB_{0.75}B'_{0.25}O_3$ (B-V_O-B and B-V_O-B') has two different oxygen vacancy sites when considering the two neighboring B-site cations bonded to the lattice oxygen and the formation energetics. For $LaB_{0.75}B'_{0.25}O_3$, we selected the most stable site that had the lower oxygen vacancy formation energy among the two sites.

Figure 2 shows the calculated oxygen vacancy formation energies for $LaB_{1-x}B'_xO_3$ (x = 0.00, 0.25, 0.50, and 0.75). We first note that the oxygen vacancy formation energies of $LaBO_3$ (the leftmost points in Fig. 2(a) to (e)) decrease in the order of B = Cr > Fe > Mn > Co > Ni. The observed trend is consistent with previously reported results from experiments[45-48] and DFT calculations.[40,41,49] Pavone *et al.*[40] explained that this trend is related to the differences in both B-O bond strengths and exothermic reduction of the B-site cations (from B^{3+} to B^{2+}) after removing an oxygen atom. In B-site doped perovskites, the values of oxygen vacancy formation energy are constrained between those of undoped perovskites ($LaBO_3$ and $LaB'O_3$). For example, the oxygen vacancy formation energy of $LaCrO_3$, which is the highest among the cases we examined here, decreases with the addition of other B-site cations instead of Cr, whereas the oxygen vacancy formation energy of $LaNiO_3$, which is the lowest among the cases, shows the opposite trend, as shown

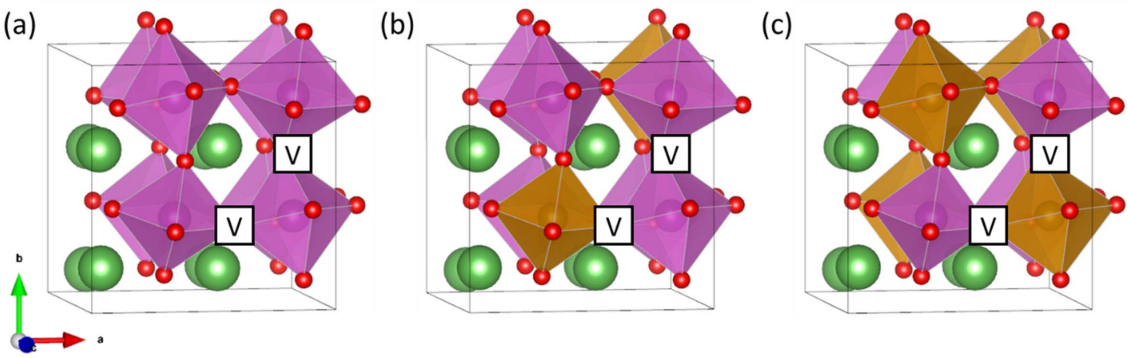

Fig. 1. Pseudocubic 2 × 2 × 2 bulk structures of (a) $LaBO_{3-\delta}$, (b) $La(B_{0.75}B'_{0.25})O_{3-\delta}$, and (c) $La(B_{0.50}B'_{0.50})O_{3-\delta}$ (B and B' = Cr, Mn, Fe, Co and Ni).

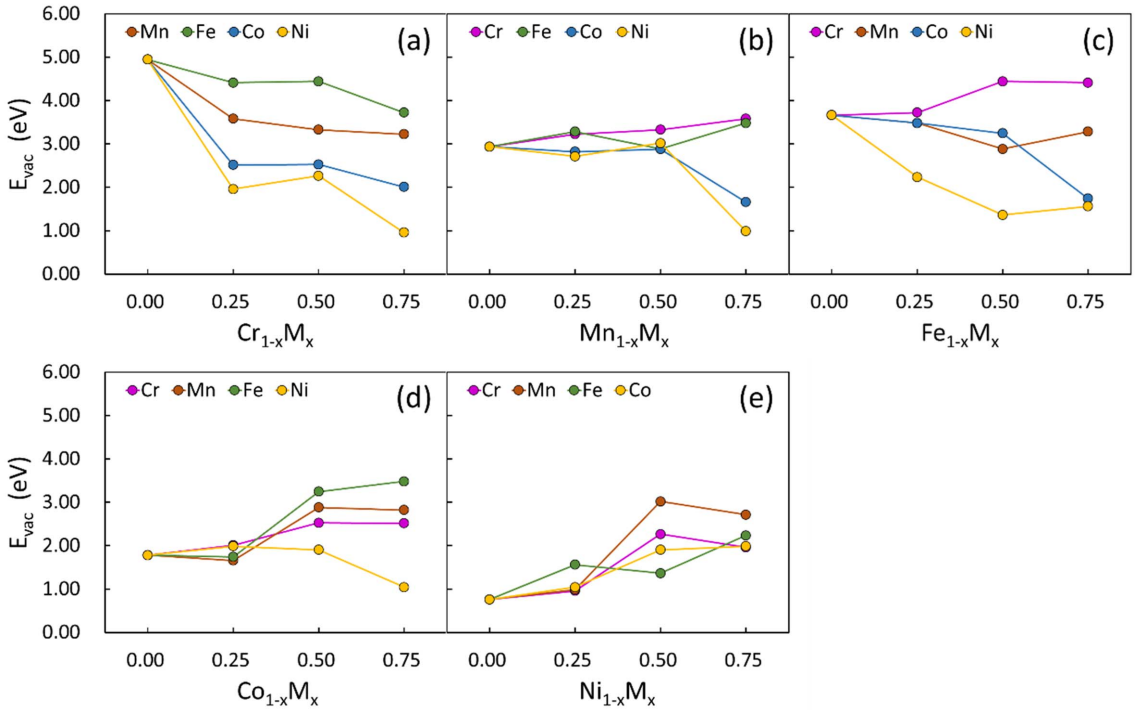

Fig. 2. Calculated oxygen vacancy formation energies (E_{vac}) for $LaB_{1-x}B'_xO_3$ (x = 0.00, 0.25, 0.50, and 0.75). Here, B = (a) Cr, (b) Mn, (c) Fe, (d) Co, and (e) Ni; B' = the other B-site cations.

in Fig. 2(a) and (e). This discrepancy may be attributed to the mixing effects of B-O bond strengths or B-site cation reduction exothermicities. These results provide a useful way of predicting oxygen vacancy formation energies: we can approximately estimate the oxygen formation energies of B-site doped perovskites from those of undoped perovskites.

3.2. Oxygen vacancy migration

The migration of oxygen vacancies follows a vacancy-mediated hopping mechanism[50] and has a curved path.[51] We therefore assumed that an oxygen vacancy passes through a triangle formed by two La atoms and a B-site cation.[16,26,51-53] Unlike $LaBO_{3-\delta}$ and $La(B_{0.50}B'_{0.50})O_{3-\delta}$, the migration barrier in $La(B_{0.75}B'_{0.25})O_{3-\delta}$ is different in accordance with the direction of the oxygen vacancy migration because there are two different oxygen vacancy sites in terms of energetics, as mentioned earlier (Fig. 3). For $La(B_{0.75}B'_{0.25})O_{3-\delta}$, we calculated the energy barriers caused by migration from a more stable to a less stable vacancy site.

Figure 4 shows the oxygen vacancy migration barriers calculated *via* the vacancy hopping mechanism. No distinct difference in the influence of B-site cations is observed compared to the oxygen vacancy formation energies. These results are consistent with previous reports on various bulk perovskites. For $LaBO_{3-\delta}$ (B = Cr, Mn, Fe, Co and Ni), the vacancy migration barriers are all similar at around 0.5 ~ 0.9 eV.[16,37,53-57] Mastrikov *et al.*[58] also reported that the oxygen vacancy migration barriers in $(La,Sr)(Co,Fe)O_{3-\delta}$ are almost independent of the chemical composition. The difference in migration barriers, therefore, may not have a significant effect on the bulk diffusion when compared to the difference in oxygen vacancy formation energies, as can be seen in Fig. 2.

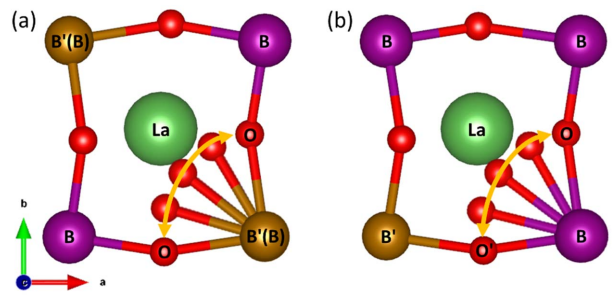

Fig. 3. 2D schematics of the curved migration pathway of an oxygen vacancy. (a) $LaBO_{3-\delta}$ and $La(B_{0.50}B'_{0.50})O_{3-\delta}$ have two identical oxygen vacancy sites and (b) $La(B_{0.75}B'_{0.25})O_{3-\delta}$ has two different oxygen vacancy sites. In (b), the oxygen vacancy migration barrier indicates the energy required to migrate from a more stable to a less stable vacancy site.

3.3. Activation energy of oxide ion (O^{2-}) bulk diffusion

The activation energy for oxide diffusion can be obtained using the sum of the oxygen vacancy formation energy (E_{vac}) and the oxygen vacancy migration energy (E_{mig}), as mentioned in Sec. 1. This implies that perovskite materials with high oxide ion diffusion rate should have low oxygen vacancy formation energy and oxygen vacancy migration

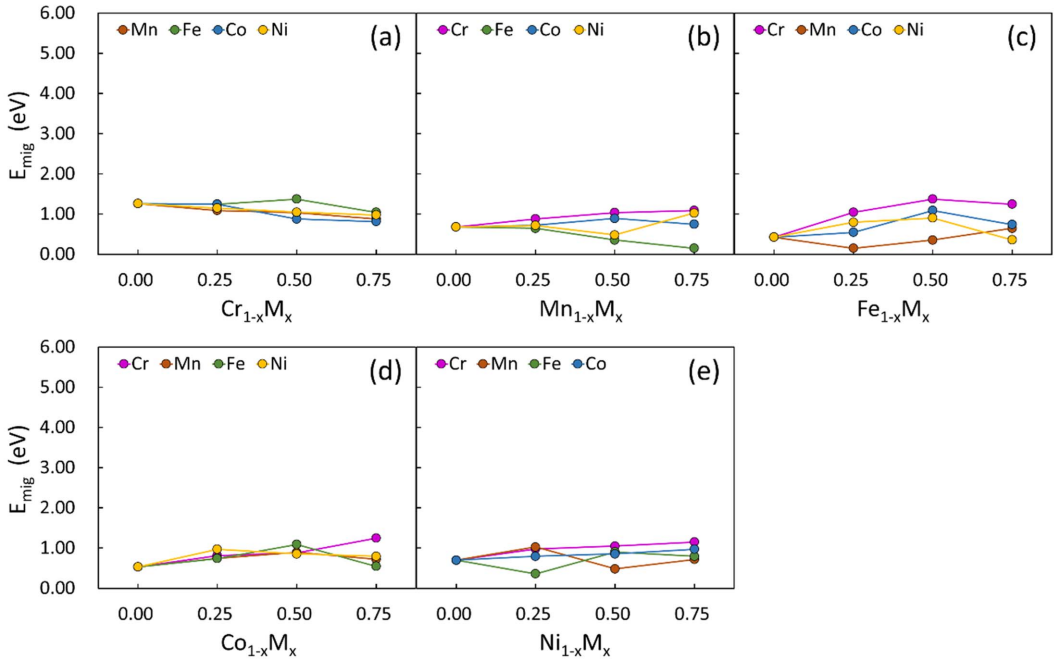

Fig. 4. Calculated oxygen vacancy migration barriers (E_{mig}) for $LaB_{1-x}B'_xO_3$ (x = 0.00, 0.25, 0.50, and 0.75). Here, B = (a) Cr, (b) Mn, (c) Fe, (d) Co, and (e) Ni; B' = the other B-site cations. The scale of the y-axis is the same as that shown in Fig. 3 for the comparison with oxygen vacancy formation energies.

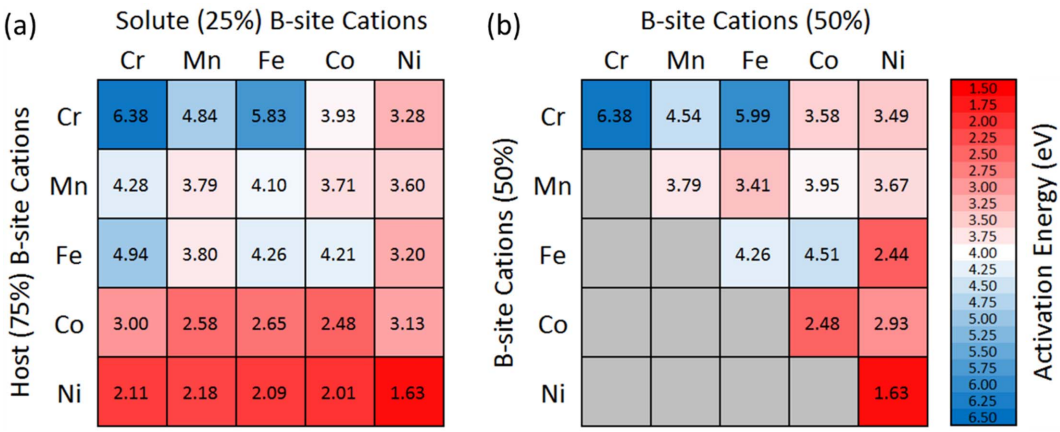

Fig. 5. Activation energies for oxide diffusion in (a) $La(B_{0.75}B'_{0.25})O_{3-\delta}$ and (b) $La(B_{0.50}B'_{0.50})O_{3-\delta}$.

energy. As mentioned in Sec. 3.2, however, in $LaBO_3$ perovskites the activation energies are mostly influenced by the oxygen vacancy formation energies. The Ni based perovskites, which easily create an oxygen vacancy, therefore have the lowest activation energies (Fig. 5). This agrees with previous experimental results that the conductivity increases as a function of Ni doping in B-sites.[59] Our results show that perovskites doped with 3*d*-late transition metals are predicted as high conductivity materials. There are, however, still other various factors that need to be considered for use as SOFC cathode materials. For example, although based on our analysis $LaNiO_3$ seems to be one of the most promising cathode materials, it may not indeed be suitable due to the instability arising from phase transformations at high temperature.[60,61] Nevertheless, our DFT results provide a principle for the fast screening of high performance SOFC cathode materials.

4. Conclusions

In this study, using DFT+U calculations, we investigated the effect of B-cation doping on bulk ionic transport in $LaB_xB'_{1-x}O_{3-\delta}$ (B, B' = Cr, Mn, Fe, Co, and Ni). The activation energy in bulk oxide diffusion were simply calculated using the summation of oxygen vacancy formation and migration energy. While oxygen vacancy formation energy generally decreased with change of B-site dopants from the middle to the late transition metals, oxygen vacancy migration energy

showed relatively independent behaviors. Comparing contributions to activation energy, we found that vacancy formation energy has a greater effect than migration energy. This implies that we can approximatively predict the activation energy simply by estimating the oxygen vacancy formation energy. Although there are many other factors that might govern the cathode performance, our results provide one set of guidelines that should be considered when designing high performance SOFC cathode materials.

Acknowledgments

The authors acknowledge financial support from the KIST Institutional Program (2E24021-13-031) and the Global Frontier R&D Program of the Center for Multiscale Energy Systems, through the National Research Foundation of Korea (NRF), funded by the Ministry of Science, ICT & Future Planning (NRF-2014M3A6A7074785); we also acknowledge supercomputing resources, including technical support, provided by the Supercomputing Center/Korea Institute of Science and Technology Information (KSC-2014-C1-003).

REFERENCES

1. N. Q. Minh, "Ceramic Fuel Cells," *J. Am. Ceram. Soc.,* **76** [3] 563-88 (1993).
2. B. C. H. Steele and A. Heinzel, "Materials for Fuel-cell Technologies," *Nature,* **414** [6861] 345-52 (2001).
3. S. M. Haile, "Fuel Cell Materials and Components," *Acta Mater.,* **51** [19] 5981-6000 (2003).
4. E. D. Wachsman and K. T. Lee, "Lowering the Temperature of Solid Oxide Fuel Cells," *Science,* **334** [6058] 935-39 (2011).
5. M. M. Kuklja, E. A. Kotomin, R. Merkle, Y. A. Mastrikov, and J. Maier, "Combined Theoretical and Experimental Analysis of Processes Determining Cathode Performance in Solid Oxide Fuel Cells," *Phys. Chem. Chem. Phys.,* **15** [15] 5443-71 (2013).
6. Y. A. Mastrikov, M. M. Kuklja, E. A. Kotomin, and J. Maier, "First-principles Modelling of Complex Perovskite $(Ba_{1-x}Sr_x)(Co_{1-y}Fe_y)O_{3-\delta}$ for Solid Oxide Fuel Cell and Gas Separation Membrane Applications," *Energy Environ. Sci.,* **3** [10] 1544-50 (2010).
7. A. B. Muñoz-García, D. E. Bugaris, M. Pavone, J. P. Hodges, A. Huq, F. Chen, H. -C. zur Loye, and E. A. Carter, "Unveiling Structure–property Relationships in $Sr_2Fe_{1.5}Mo_{0.5}O_{6-\delta}$, an Electrode Material for Symmetric Solid Oxide Fuel Cells," *J. Am. Chem. Soc.,* **134** [15] 6826-33 (2012).
8. Z. Wang, R. Peng, W. Zhang, X. Wu, C. Xia, and Y. Lu, "Oxygen Reduction and Transport on the $La_{1-x}Sr_xCo_{1-y}Fe_yO_{3-\delta}$ Cathode in Solid Oxide Fuel Cells: A First-principles Study," *J. Mater. Chem. A,* **1** [41] 12932-40 (2013).
9. S. B. Adler, "Factors Governing Oxygen Reduction in Solid Oxide Fuel Cell Cathodes," *Chem. Rev.,* **104** 4791–844 (2004).
10. S. B. Adler, "Electrode Kinetics of Porous Mixed-conducting Oxygen Electrodes," *J. Electrochem. Soc.,* **143** [11] 3554 (1996).
11. S. B. Adler, "Mechanism and Kinetics of Oxygen Reduction on Porous $La_{1-x}Sr_xCoO_{3-\delta}$ Electrodes," *Solid State Ionics,* **111** [1-2] 125-34 (1998).
12. S. Choi, S. Yoo, J. Kim, S. Park, A. Jun, S. Sengodan, J. Kim, J. Shin, H. Y. Jeong, Y. -M. Choi, G. Kim, and M. Liu, "Highly Efficient and Robust Cathode Materials for Low-temperature Solid Oxide Fuel Cells: $PrBa_{0.5}Sr_{0.5}Co_{2-x}Fe_xO_{5+\delta}$," *Sci. Rep.,* **3** (2013).
13. S. Bao, C. Ma, G. Chen, X. Xu, E. Enriquez, C. Chen, Y. Zhang, J. L. Bettis Jr., M. -H. Whangbo, C. Dong, and Q. Zhang, "Ultrafast Atomic Layer-by-layer Oxygen Vacancy-exchange Diffusion in Double-perovskite $LnBaCo_2O_{5.5+\delta}$ Thin Films," *Sci. Rep.,* **4** 4726 (2014).
14. C. N. Munnings, S. J. Skinner, G. Amow, P. S. Whitfield, and I. J. Davidson, "Oxygen Transport in the $La_2Ni_{1-x}Co_xO_{4+\delta}$ System," *Solid State Ionics,* **176** [23-24] 1895-901 (2005).
15. E. Boehm, J. -M. Bassat, P. Dordor, F. Mauvy, J. -C. Grenier, and Ph. Stevens, "Oxygen Diffusion and Transport Properties in Non-stoichiometric $Ln_{2-x}NiO_{4+\delta}$ Oxides," *Solid State Ionics,* **176** [37-38] 2717-25 (2005).
16. J. W. Han and B. Yildiz, "Enhanced One Dimensional Mobility of Oxygen on Strained $LaCoO_3$(001) Surface," *J. Mater. Chem.,* **21** [47] 18983 (2011).
17. H. Jalili, J. W. Han, Y. Kuru, Z. Cai, and B. Yildiz, "New Insights into the Strain Coupling to Surface Chemistry, Electronic Structure, and Reactivity of $La_{0.7}Sr_{0.3}MnO_3$," *J. Phys. Chem. Lett.,* **2** [7] 801-7 (2011).
18. Z. Cai, Y. Kuru, J. W. Han, Y. Chen, and B. Yildiz, "Surface Electronic Structure Transitions at High Temperature on Perovskite Oxides: The Case of Strained $La_{0.8}Sr_{0.2}CoO_3$ Thin Films," *J. Am. Chem. Soc.,* **133** [44] 17696-704 (2011).
19. M. Kubicek, Z. Cai, W. Ma, B. Yildiz, H. Hutter, and J. Fleig, "Tensile Lattice Strain Accelerates Oxygen Surface Exchange and Diffusion in $La_{1-x}Sr_xCoO_{3-\delta}$ Thin Films," *ACS Nano,* **7** [4] 3276-86 (2013).
20. J. L. M. Rupp, E. Fabbri, D. Marrocchelli, J. W. Han, D. Chen, E. Traversa, H. L. Tuller, and B. Yildiz, "Scalable Oxygen-ion Transport Kinetics in Metal-oxide Films: Impact of Thermally Induced Lattice Compaction in Acceptor Doped Ceria Films," *Adv. Funct. Mater.,* **24** [11] 1562-74 (2014).
21. X. Yue, A. Yan, M. Zhang, L. Liu, Y. Dong, and M. Chen, "Investigation on Scandium-Doped Manganate $La_{0.8}Sr_{0.2}Mn_{1-x}Sc_xO_{3-\delta}$ Cathode for Intermediate Temperature Solid Oxide Fuel Cells," *J. Power Sources,* **185** [2] 691-97 (2008).
22. V. Dusastre and J. A. Kilner, "Optimisation of Composite Cathodes for Intermediate Temperature SOFC Applications," *Solid State Ionics,* **126** [1-2] 163-74 (1999).
23. B. C. H. Steele, "Survey of Materials Selection for Ceramic Fuel Cells II. Cathodes and Anodes," *Solid State Ionics,* **86-88** 1223-34 (1996).
24. H. L. Tuller, "Semiconduction and Mixed Ionic-electronic Conduction in Nonstoichiometric Oxides: Impact and Control," *Solid State Ionics,* **94** [1-4] 63-74 (1997).
25. M. Cherry, M. S. Islam, and C. R. A. Catlow, "Oxygen Ion Migration in Perovskite-type Oxides," *J. Solid State Chem.,* **118** [1] 125-32 (1995).

26. A. M. Ritzmann, A. B. Muñoz-García, M. Pavone, J. A. Keith, and E. A. Carter, "Ab Initio DFT+U Analysis of Oxygen Vacancy Formation and Migration in $La_{1-x}Sr_xFeO_{3-\delta}$ (x = 0, 0.25, 0.50)," *Chem. Mater.,* **25** [15] 3011-19 (2013).
27. A. B. Muñoz-García, M. Pavone, A. M. Ritzmann, and E. A. Carter, "Oxide Ion Transport in $Sr_2Fe_{1.5}Mo_{0.5}O_{6-\delta}$, A Mixed Ion-electron Conductor: New Insights from First Principles Modeling," *Phys. Chem. Chem. Phys.,* **15** [17] 6250-59 (2013).
28. A. B. Muñoz-García, A. M. Ritzmann, M. Pavone, J. A. Keith, and E. A. Carter, "Oxygen Transport in Perovskite-type Solid Oxide Fuel Cell Materials: Insights from Quantum Mechanics," *Acc. Chem. Res.,* **47** [11] 3340-48 (2014).
29. G. Kresse and J. Furthmüller, "Efficient Iterative Schemes for Ab Initio Total-energy Calculations Using a Plane-wave Basis Set," *Phys. Rev. B,* **54** [16] 11169-86 (1996).
30. G. Kresse and J. Furthmüller, "Efficiency of Ab-initio Total Energy Calculations for Metals and Semiconductors Using a Plane-wave Basis Set," *Comput. Mater. Sci.,* **6** [1] 15-50 (1996).
31. J. P. Perdew, K. Burke, and M. Ernzerhof, "Generalized Gradient Approximation Made Simple," *Phys. Rev. Lett.,* **77** [18] 3865-68 (1996).
32. E. A. Carter, "Challenges in Modeling Materials Properties without Experimental Input," *Science,* **321** [5890] 800-3 (2008).
33. S. L. Dudarev, G. A. Botton, S. Y. Savrasov, C. J. Humphreys, and A. P. Sutton, "Electron-energy-loss Spectra and the Structural Stability of Nickel Oxide: An LSDA+U Study," *Phys. Rev. B,* **57** [3] 1505-9 (1998).
34. L. Wang, T. Maxisch, and G. Ceder, "Oxidation Energies of Transition Metal Oxides within the GGA+U Framework," *Phys. Rev. B,* **73** [19] 195107 (2006).
35. H. J. Monkhorst and J. D. Pack, "Special Points for Brillouin-zone Integrations," *Phys. Rev. B,* **13** [12] 5188-92 (1976).
36. Y. -L. Lee and D. Morgan, "Ab Initio Defect Energetics of Perovskite (001) Surfaces for Solid Oxide Fuel Cells: A Comparative Study of $LaMnO_3$ versus $SrTiO_3$ and $LaAlO_3$," *Phys. Rev. B,* **91** [19] 195430 (2015).
37. T. Mayeshiba and D. Morgan, "Strain Effects on Oxygen Migration in Perovskites," *Phys. Chem. Chem. Phys.,* **17** [4] 2715-21 (2015).
38. Y. -L. Lee, J. Kleis, J. Rossmeisl, Y. Shao-Horn, and D. Morgan, "Prediction of Solid Oxide Fuel Cell Cathode Activity with First-principles Descriptors," *Energy Environ. Sci.,* **4** [10] 3966–70 (2011).
39. J. Ko, H. Kwon, H. Kang, B. -K. Kim, and J. W. Han, "Universality in Surface Mixing Rule of Adsorption Strength for Small Adsorbates on Binary Transition Metal Alloys," *Phys. Chem. Chem. Phys.,* **17** [5] 3123-30 (2015).
40. M. Pavone, A. M. Ritzmann, and E. A. Carter, "Quantum-mechanics-based Design Principles for Solid Oxide Fuel Cell Cathode Materials," *Energy Environ. Sci.,* **4** [12] 4933-37 (2011).
41. A. M. Deml, V. Stevanović, C. L. Muhich, C. B. Musgrave, and O'Hayre "Oxide Enthalpy of Formation and Band Gap Energy as Accurate Descriptors of Oxygen Vacancy Formation Energetics," *Energy Environ. Sci.,* **7** [6] 1996-2004 (2014).
42. G. Henkelman, B. P. Uberuaga, and H. Jónsson, "A Climbing Image Nudged Elastic Band Method for Finding Saddle Points and Minimum Energy Paths," *J. Chem. Phys.,* **113** [22] 9901 (2000).
43. D. Sheppard, R. Terrell, and G. Henkelman, "Optimization Methods for Finding Minimum Energy Paths," *J. Chem. Phys.,* **128** [13] 134106 (2008).
44. J. W. Han and B. Yildiz, "Mechanism for Enhanced Oxygen Reduction Kinetics at the $(La,Sr)CoO_{3-\delta}/(La,Sr)_2CoO_{4+\delta}$ Hetero-interface," *Energy Environ. Sci.,* **5** [9] 8598–607 (2012).
45. J. H. Kuo, H. U. Anderson, and D. M. Sparlin, "Oxidation-reduction Behavior of Undoped and Sr-Doped $LaMnO_3$ Nonstoichiometry and Defect Structure," *J. Solid State Chem.,* **83** [1] 52-60 (1989).
46. J. Nowotny and M. Rekas, "Defect Chemistry of (La,Sr) MnO_3," *J. Am. Ceram. Soc.,* **81** [1] 67-80 (1998).
47. J. Mizusaki, M. Yoshihiro, S. Yamauchi, and K. Fueki, "Nonstoichiometry and Defect Structure of the Perovskite-type Oxides $La_{1-x}Sr_xFeO_{3-\delta}$," *J. Solid State Chem.,* **58** [2] 257-66 (1985).
48. J. Mizusaki, Y. Mima, S. Yamauchi, and K. Fueki, "Nonstoichiometry of the Perovskite-type Oxides $La_{1-x}Sr_xCoO_{3-\delta}$," *J. Solid State Chem.,* **80** [1] 102-111 (1989).
49. Y. -L. Lee, K. Kleis, J. Rossmeisl, and D. Morgan, "Ab Initio Energetics of $LaBO_3$(001) (B = Mn, Fe, Co, and Ni) for Solid Oxide Fuel Cell Cathodes," *Phys. Rev. B,* **80** [22] 224101 (2009).
50. M. S. Islam, "Computer Modelling of Defects and Transport in Perovskite Oxides," *Solid State Ionics,* **154-155** 75-85 (2002).
51. A. Jones and M. S. Islam, "Atomic-scale Insight into $LaFeO_3$ Perovskite: Defect Nanoclusters and Ion Migration," *J. Phys. Chem. C,* **112** [12] 4455-62 (2008).
52. J. A. Kilner and R. J. Brook, "A Study of Oxygen Ion Conductivity in Doped Non-stoichiometric Oxides," *Solid State Ionics,* **6** [3] 237-52 (1982).
53. M. S. Islam, "Ionic Transport in ABO_3 Perovskite Oxides: A Computer Modelling Tour," *J. Mater. Chem.,* **10** [4] 1027-38 (2000).
54. T. Ishigaki, S. Yamauchi, J. Mizusaki, K. Kueki, and H. Tamura, "Tracer Diffusion Coefficient of Oxide Ions in $LaCoO_3$ Single Crystal," *J. Solid State Chem.,* **54** [1] 100-7 (1984).
55. T. Ishigaki, S. Yamauchi, K. Kishio, J. Mizusaki, and K. Fueki, "Diffusion of Oxide Ion Vacancies in Perovskite-type Oxides," *J. Solid State Chem.,* **73** [1] 179-87 (1988).
56. S. Carter, A. Selcuk, R. J. Chater, J. Kajda, J. A. Kilner, and B. C. H. Steele, "Oxygen Transport in Selected Nonstoichiometric Perovskite-structure Oxides," *Solid State Ionics,* **53-56** 597-605 (1992).
57. I. Yasuda and M. Hishinuma, "Electrical Conductivity and Chemical Diffusion Coefficient of Strontium-doped Lanthanum Manganites," *J. Solid State Chem.,* **123** [2] 382-90 (1996).
58. Y. A. Mastrikov, R. Merkle, E. A. Kotomin, M. M. Kuklja, and J. Maier, "Formation and Migration of Oxygen Vacancies in $La_{1-x}Sr_xCo_{1-y}Fe_yO_{3-\delta}$ Perovskites: Insight from Ab Initio Calculations and Comparison with $Ba_{1-x}Sr_xCo_{1-y}Fe_yO_{3-\delta}$," *Phys. Chem. Chem. Phys.,* **15** [3] 911-18 (2013).

59. V. V. Kharton, A. P. Viskup, D. M. Bochkov, E. N. Naumovich, and O. P. Reut, "Mixed Electronic and Ionic Conductivity of $LaCo(M)O_3$ (M = Ga, Cr, Fe or Ni): III. Diffusion of Oxygen through $LaCo_{1-x-y}Fe_xNi_yO_{3\pm\delta}$ Ceramics," *Solid State Ionics,* **110** [1-2] 61-68 (1998).
60. M. Zinkevich and F. Aldinger, "Thermodynamic Analysis of the Ternary La-Ni-O System," *J. Alloys Compd.,* **375** [1-2] 147-61 (2004).
61. E. V. Tsipis, E. A. Kiselev, V. A. Kolotygin, J. C. Waerenborgh, V. A. Cherepanov, and V. V. Kharton, "Mixed Conductivity, Mössbauer Spectra and Thermal Expansion of $(La,Sr)(Fe,Ni)O_{3-\delta}$ Perovskites," *Solid State Ionics,* **179** [38] 2170-80 (2008).